Arab. J. Math. (2020) 9:19–36
https://doi.org/10.1007/s40065-019-0237-9
Arabian Journal of Mathematics

Shelly Arora · Inderpreet Kaur · Wudneh Tilahun

An exploration of quintic Hermite splines to solve Burgers' equation

Received: 10 July 2018 / Accepted: 8 January 2019 / Published online: 18 January 2019

Abstract An innovative scheme of collocation having quintic Hermite splines as base functions has been followed to solve Burgers' equation. The scheme relies on approximation of Burgers' equation directly in non-linear form without using Hopf–Cole transformation (Hopf in Commun Pure Appl Math 3:201–216, 1950; Cole in Q Appl Math 9:225–236, 1951). The significance of the numerical technique is demonstrated by comparing the numerical results to the exact solution and published results (Asaithambi in Appl Math Comput 216:2700–2708, 2010; Mittal and Jain in Appl Math Comput 218:7839–7855, 2012). Five problems with different initial conditions have been examined to validate the efficiency and accuracy of the scheme. Euclidean and supremum norms have been reckoned to scrutinize the stability of the numerical scheme. Results have been demonstrated in plane and surface plots to indicate the effectiveness of the scheme.

Mathematics Subject Classification 35B25 · 65N35 · 65N12

1 Introduction

Burgers' equation is a partial differential equation that was originally proposed as a simplified model of turbulence as exhibited by the full-fledged Navier–Stokes equations. It is a non-linear equation for which exact solutions are available [10,16] and is therefore important as a benchmark problem for numerical methods. It has been found to describe distinct phenomena such as a mathematical model of turbulence [8] and the approximate theory of flow through a shock wave traveling in a viscous fluid [10]. The occurrence of non-linear term and of higher order derivatives with small coefficients in both of Burgers' equation and Navier–Stokes equation are similar [27]. Burgers' equation is the simplified form of Navier–Stokes equation which does not involve stress term.

Burgers' equation arises frequently in various processes such as turbulence, elasticity, heat conduction processes, shock wave theory, and fluid and gas dynamic processes. It specifies the correlation between convection and diffusion.

Burgers' equation has been solved by using a variety of numerical methods such as modified Adomian method [1], homotopy analysis method [17], finite difference scheme [18,20,22,28], automatic differenti-

S. Arora · I. Kaur (✉)
Department of Mathematics, Punjabi University, Patiala, Punjab 147002, India
E-mail: inder3003@gmail.com

S. Arora
E-mail: aroshelly@gmail.com

W. Tilahun
Department of Mathematics, Debre Tabor University, Debre Tabor, Ethiopia
E-mail: wud2hagie@gmail.com

ation [7], finite element method [2], and spline collocation [6,11,19,25,27,31]. Several investigators have solved Burgers' equation by transforming the non-linear term into linear one [18,20,27,28] using Hopf–Cole transformation [10,16].

In the present study, a numerical solution of Burgers' equation has been achieved by applying quintic Hermite collocation method directly, i.e., without transforming the non-linear term into linear one using Hopf–Cole transformation.

Fundamentally, the non-linear Burgers' equation is of the form:

$$\frac{\partial u}{\partial t} = \varepsilon \frac{\partial^2 u}{\partial x^2} - u\frac{\partial u}{\partial x}; \quad (x,t) \in \Omega \times (0,T). \tag{1}$$

Initially,

$$u(x,0) = u_0(x); \quad \forall x \in \Omega. \tag{2}$$

Boundary conditions can be defined as:

$$u(p,t) = g_1(t) \quad \text{and} \quad u(q,t) = g_2(t); \quad \forall t \in (0,T). \tag{3}$$

Cole [10] has solved the Burgers' equation in linear heat equation form, which can be presented as

$$\frac{\partial \theta}{\partial t} = \varepsilon \frac{\partial^2 \theta}{\partial x^2}. \tag{4}$$

If $\theta(x,t)$ is the solution of Eq. (4), then

$$u(x,t) = -2\varepsilon \frac{\theta_x}{\theta} \tag{5}$$

is the solution of non-linear form of Burgers' equation represented by Eq. (1). Using the initial and boundary conditions given in [10], the solution of Burgers' equation has been presented as:

$$u(x,t) = \frac{2\varepsilon\pi}{k} \frac{\sum_{n=1}^{\infty} \exp[-\varepsilon n^2\pi^2 t/k^2] n R_n \sin(n\pi x)/k}{R_0 + \sum_{n=1}^{\infty} \exp[-\varepsilon n^2\pi^2 t/k^2] R_n \cos(n\pi x)/k}. \tag{6}$$

The solution presented in Eq. (6) involves complex trigonometric as well as exponential functions which are time consuming and difficult to solve.

In the present study, the Burgers' equation with ε as viscosity parameter, has been solved numerically using quintic Hermite collocation method. It has been elucidated in different forms using distinct initial conditions in terms of constant, and polynomial and trigonometric functions.

2 Quintic Hermite collocation method (QHCM)

The orthogonal collocation is one of the weighted residual methods which is used to release the differential equation and the boundary adjoining it. It is one of the simplest methods to discretize the boundary value problems. In this procedure, an interpolating polynomial can be chosen as a base function to estimate the trial function and then get the residual. A Lagrangian interpolating polynomial can be taken as trial function which discretizes the unknown function and can be represented by a series of orthogonal polynomials. The residual is defined over its region and is set equal to zero at collocation points.

The quintic Hermite collocation is one of the Hermite collocation methods [3–5,12–14,21,23,24,26,29,32] in which the base function is designated to be the Hermite interpolating polynomials. It is the combination of the orthogonal collocation and the finite element method. In Hermite collocation, the evaluation function is approximated by Hermite interpolating polynomial of order $2k+1$ ($k > 0$). It is the generalization of Lagrange interpolation with polynomials that not only interpolate the function at each node but also its consecutive derivatives. In the present study, quintic Hermite polynomials of order 5, i.e., $k = 2$, have been taken as base function to approximate the trial function. It consists of four node points.

Quintic Hermite interpolating polynomials can be expressed in the following form [9]:

$$u(x,t)=\sum_{j=1}^{6}P_j(x)p(x_j)+\bar{P}_j(x)p'(x_j)+\bar{\bar{P}}_j(x)p''(x_j);\quad x\in[x_{i-1},x_{i+1}], \tag{7}$$

where $p(x_j)$, $p'(x_j)$ and $p''(x_j)$ are quintic Hermite coefficients and $P_j(x)$, $\bar{P}_j(x)$ and $\bar{\bar{P}}_j(x)$ are quintic Hermite interpolating polynomials which can be expressed as:

$$P_j(x)=\begin{cases}6\left(\frac{x_{i+1}-x}{x_{i+1}-x_i}\right)^5-15\left(\frac{x_{i+1}-x}{x_{i+1}-x_i}\right)^4+10\left(\frac{x_{i+1}-x}{x_{i+1}-x_i}\right)^3, & x_i\le x\le x_{i+1}\\ 6\left(\frac{x-x_{i-1}}{x_i-x_{i-1}}\right)^5-15\left(\frac{x-x_{i-1}}{x_i-x_{i-1}}\right)^4+10\left(\frac{x-x_{i-1}}{x_i-x_{i-1}}\right)^3, & x_{i-1}\le x\le x_i\\ 0, & \text{elsewhere,}\end{cases} \tag{8}$$

$$\bar{P}_j(x)=\begin{cases}3\frac{(x_{i+1}-x)^5}{(x_{i+1}-x_i)^4}-7\frac{(x_{i+1}-x)^4}{(x_{i+1}-x_i)^3}+4\frac{(x_{i+1}-x)^3}{(x_{i+1}-x_i)^2}, & x_i\le x\le x_{i+1}\\ -3\frac{(x-x_{i-1})^5}{(x_i-x_{i-1})^4}+7\frac{(x-x_{i-1})^4}{(x_i-x_{i-1})^3}-4\frac{(x-x_{i-1})^3}{(x_i-x_{i-1})^2}, & x_{i-1}\le x\le x_i\\ 0, & \text{elsewhere,}\end{cases} \tag{9}$$

$$\bar{\bar{P}}_j(x)=\begin{cases}0.5\frac{(x_{i+1}-x)^5}{(x_{i+1}-x_i)^3}-\frac{(x_{i+1}-x)^4}{(x_{i+1}-x_i)^2}+0.5\frac{(x_{i+1}-x)^3}{(x_{i+1}-x_i)}, & x_i\le x\le x_{i+1}\\ 0.5\frac{(x-x_{i-1})^5}{(x_i-x_{i-1})^3}-\frac{(x-x_{i-1})^4}{(x_i-x_{i-1})^2}+0.5\frac{(x-x_{i-1})^3}{(x_i-x_{i-1})}, & x_{i-1}\le x\le x_i\\ 0, & \text{elsewhere,}\end{cases} \tag{10}$$

where

$$\begin{aligned}&P_j(x_i)=\delta_{ij},\quad P_j^{'}(x_i)=0,\quad P_j^{''}(x_i)=0,\quad i,j=1,2,\ldots,6\\ &\bar{P}_j(x_i)=0,\quad \bar{P}_j^{'}(x_i)=\delta_{ij},\quad \bar{P}_j^{''}(x_i)=0,\quad i,j=1,2,\ldots,6\\ &\bar{\bar{P}}_j(x_i)=0,\quad \bar{\bar{P}}_j^{'}(x_i)=0,\quad \bar{\bar{P}}_j^{''}(x_i)=\delta_{ij},\quad i,j=1,2,\ldots,6.\end{aligned}$$

In quintic Hermite collocation method, the global domain is divided into subdomains called finite elements. The solution can be initiated approximately on these elements, to acquire the numerical values up to a certain degree of accuracy.

The principle of collocation is then applied within each sub-domain by instigating a new variable $\xi=\frac{x-x_\gamma}{h_\gamma}$, where $h_\gamma=x_{\gamma+1}-x_\gamma$, $\xi=0$ at $x=x_\gamma$ and ξ=1 at $x=x_{\gamma+1}$. At jth collocation point, $x_j=\xi_j h_\gamma+x_\gamma$. After rearranging the terms $P_j(x)$, $\bar{P}_j(x)$ and $\bar{\bar{P}}_j(x)$ can be rewritten as:

$$\begin{aligned}H_1&=\left(1-10\xi^3+15\xi^4-6\xi^5\right),\\ H_2&=h_\gamma\left(\xi-6\xi^3+8\xi^4-3\xi^5\right),\\ H_3&=h_\gamma^2\left(0.5\xi^2-1.5\xi^3+1.5\xi^4-0.5\xi^5\right),\\ H_4&=h_\gamma^2\left(0.5\xi^3-\xi^4+0.5\xi^5\right),\\ H_5&=\left(10\xi^3-15\xi^4+6\xi^5\right),\\ H_6&=h_\gamma\left(-4\xi^3+7\xi^4-3\xi^5\right).\end{aligned} \tag{11}$$

These quintic Hermite interpolating polynomials also satisfy the relations $H_1(\xi)=H_5(1-\xi)$, $H_2(\xi)=-H_6(1-\xi)$, $H_3(\xi)=H_4(1-\xi)$.

Hence, the trial function takes the following form:

$$u^\gamma(\xi,t)=\sum_{i=1}^{6}\nu_i^\gamma(t)H_i(\xi), \tag{12}$$

where $\nu_i's$ are continuous functions of t.

Details of graphical representation and structure of elements in QHCM using quintic Hermite interpolating polynomials are given in [3].

3 Implementation of QHCM

The system of equations defined by Eqs. (1)–(3) has been discretized using QHCM at jth collocation point. The system of discretized equations can be expressed as:

$$\sum_{i=1}^{6} \frac{\mathrm{d}\nu_i^{\gamma}}{\mathrm{d}t} H_i(\xi_j) = \frac{\varepsilon}{h_{\gamma}^2} \sum_{i=1}^{6} \nu_i^{(\gamma)} H_i''(\xi_j) - \frac{1}{h_{\gamma}} \sum_{i=1}^{6} \nu_i^{(\gamma)} H_i'(\xi_j) \times \sum_{i=1}^{6} \nu_i^{(\gamma)} H_i(\xi_j). \tag{13}$$

Initially,

$$u(x_{\gamma} + \xi_j h_{\gamma}, 0) = u_0(x_{\gamma} + \xi_j h_{\gamma}). \tag{14}$$

At boundaries,

$$u^1(\xi_1, t) = g_1(t) \quad \text{and} \quad u^{ne}(\xi_6, t) = g_2(t), \tag{15}$$

where $j = 2, 3, 4, 5$ and $\gamma = 1, 2, \ldots, ne$.

After discretization, Burgers' equation has been solved using MATLAB with $'ode15s'$ system solver which uses backward differentiation formula to solve the system of non-linear differential equations.

4 Stability analysis

Let $E = u(x,t) - u^{\gamma}$, where E defines the pointwise error, $u(x,t)$ being the exact solution and u^{γ} is the approximate solution obtained by quintic Hermite collocation method.

Stability of the numerical method has been checked by Euclidean norm and supremum norm interpreted by the formula given below:

$$\begin{aligned} ||U||_2 &= \sqrt{\sum_{\gamma=1}^{ne} h_{\gamma} \sum_{i=1}^{6} w_i (E_i)^2} \\ &= \sqrt{\sum_{\gamma=1}^{ne} h_{\gamma} \sum_{i=1}^{6} w_i (u(x_i,t) - u_i^{\gamma})^2}, \end{aligned} \tag{16}$$

where E_i is the pointwise error, $w_i's$ are the corresponding weight functions and h_{γ} is the length of the γth subdomain.

$$||U||_{\infty} = \max_{x_i} |E_i| = \max_{x_i} |u(x_i,t) - u_i^{\gamma}|, \quad \forall\, i = 1, 2, \ldots, 6 \quad \text{and} \quad \gamma = 1, 2, \ldots, ne \tag{17}$$

The order of convergence has been determined by the following lemma.

Lemma 4.1 [3,4,15] *Let H is the interpolating polynomial of function u defined on $[a,b]$, such that H is related to the space of quintic Hermite interpolating polynomials. Then the order of convergence of quintic Hermite interpolation technique is defined to be:*

$$||u^{(j)} - H^{(j)}|| \leq C||u^{(6-j)}||h^{6-j}, \quad j = 0, 1, \ldots, 5, \tag{18}$$

where C is the generic constant.

The detailed proof of the above lemma is given in [3].

Table 1 Comparison of numerical values with exact ones as well as with published results [7,25] for $\varepsilon = 1$, $\sigma = 2$ and $t = 0.001$

ξ	Present method	[25]	[7]	Exact solution
0.1	0.653545	0.653547	0.653589	0.653544
0.2	1.305534	1.305540	1.305611	1.305534
0.3	1.949364	1.949376	1.949485	1.949364
0.4	2.565925	2.565949	2.566103	2.565925
0.5	3.110739	3.110778	3.110992	3.110739
0.6	3.492866	3.492910	3.493222	3.492866
0.7	3.549595	3.549585	3.550079	3.549595
0.8	3.050134	3.049957	3.050702	3.050134
0.9	1.816660	1.816379	1.817077	1.816660
$\|\|U\|\|_2$	3.29704×10^{-8}	1.07×10^{-4}	–	–
$\|\|U\|\|_\infty$	5.00000×10^{-7}	2.85×10^{-4}	–	–

Table 2 Comparison of numerical values with exact ones as well as with published results [7,25] for $\varepsilon = 0.5$, $\sigma = 2$ and $t = 0.001$

ξ	Present method	[25]	[7]	Exact solution
0.1	0.327870	0.327870	0.327874	0.327870
0.2	0.655069	0.655071	0.655078	0.655069
0.3	0.978413	0.978416	0.978427	0.978413
0.4	1.288463	1.288469	1.288485	1.288463
0.5	1.563064	1.563074	1.563096	1.563064
0.6	1.756642	1.756654	1.756691	1.756642
0.7	1.787206	1.787204	1.787281	1.787206
0.8	1.537694	1.537649	1.537794	1.537694
0.9	0.916860	0.916786	0.916941	0.916860
$\|\|U\|\|_2$	4.61585×10^{-8}	2.79×10^{-5}	–	–
$\|\|U\|\|_\infty$	5.00000×10^{-7}	7.44×10^{-5}	–	–

5 Numerical examples

5.1 Problem

Burgers' equation defined by Eq. (1) is solved for initial condition

$$(x, 0) = \frac{2\varepsilon\pi \sin \pi x}{\sigma + \cos \pi x}, \quad \text{where} \quad \sigma > 1. \tag{19}$$

Boundary conditions are taken to be Dirichlet's.

At jth collocation point and γth element, the initial and boundary conditions can be expressed as:

$$u(x_\gamma + \xi_j h_\gamma, 0) = \frac{2\varepsilon\pi \sin \pi(x_\gamma + \xi_j h_\gamma)}{\sigma + \cos \pi(x_\gamma + \xi_j h_\gamma)}, \quad \forall \xi_j \in (0, 1) \tag{20}$$

$$u(0, t) = 0 \text{ and } u(1, t) = 0 \quad \forall\, t > 0. \tag{21}$$

This problem has been deciphered using the quintic Hermite collocation method. The numerically obtained results have been compared to exact ones as well as to the published results [7,25] for different values of ε, i.e., $\varepsilon = 1, 0.5, 0.2, 0.1$, $\sigma = 2$ and at $t = 0.001$. The comparison of numerically calculated values using QHCM has been done with automatic differentiation method [7], modified cubic B-spline collocation method [25] and exact solution [30]. This comparison of numerical values is revealed in Tables 1, 2, 3 and 4.

Euclidean as well as supremum norms have also been enumerated using formulae given in Eqs. (16) and (17). It can be observed from these tables that QHCM agrees well with the exact solution as compared to other approaches discussed here [7,25]. Also Euclidean and supremum norms determined by QHCM have been collated to [25], which are presented in Tables 1, 2, 3 and 4. It has been remarked that the norms measured by the present method are better than those given by [25].

The collation of Euclidean and supremum norms for $\gamma = 10, 20, 40$ has also been done. These norms have been assessed for $\varepsilon = 0.01$, $\sigma = 100$ and $t = 0.001$ which are presented in Table 5. In Table 6, these

Table 3 Comparison of numerical values with exact ones as well as with published results [7,25] for $\varepsilon = 0.2$, $\sigma = 2$ and $t = 0.001$

ξ	Present method	[25]	[7]	Exact solution
0.1	0.131412	0.131412	0.131412	0.131412
0.2	0.262581	0.262581	0.262582	0.262581
0.3	0.392262	0.392263	0.392263	0.392262
0.4	0.516710	0.516710	0.516711	0.516710
0.5	0.627080	0.627081	0.627082	0.627079
0.6	0.705120	0.705122	0.705124	0.705120
0.7	0.717882	0.717882	0.717890	0.717882
0.8	0.618137	0.618129	0.618148	0.618136
0.9	0.368814	0.368802	0.368824	0.368814
$\|\|U\|\|_2$	7.66163×10^{-8}	4.57×10^{-6}	–	–
$\|\|U\|\|_\infty$	5.00000×10^{-7}	1.22×10^{-5}	–	–

Table 4 Comparison of numerical values with exact ones as well as with published results [7,25] for $\varepsilon = 0.1$, $\sigma = 2$ and $t = 0.001$

ξ	Present method	[25]	[7]	Exact solution
0.1	0.065750	0.065750	0.065750	0.065750
0.2	0.131383	0.131383	0.131383	0.131383
0.3	0.196281	0.196281	0.196281	0.196281
0.4	0.258576	0.258576	0.258576	0.258576
0.5	0.313849	0.313850	0.313850	0.313849
0.6	0.352972	0.352972	0.352972	0.352972
0.7	0.359443	0.359443	0.359444	0.359443
0.8	0.309580	0.309579	0.309583	0.309580
0.9	0.184754	0.184751	0.184756	0.184754
$\|\|U\|\|_2$	5.22391×10^{-8}	1.15×10^{-6}	–	–
$\|\|U\|\|_\infty$	4.00000×10^{-7}	3.08×10^{-6}	–	–

Table 5 Comparison of $||U||_\infty$ and $||U||_2$ norms with published results [25] for $\varepsilon = 0.01$, $\sigma = 100$ and $t = 0.001$

γ	Present method	[25]	Present method	[25]
	$\|\|U\|\|_\infty$	$\|\|U\|\|_\infty$	$\|\|U\|\|_2$	$\|\|U\|\|_2$
10	4.1212×10^{-7}	4.6280×10^{-7}	5.4357×10^{-8}	3.2840×10^{-7}
20	1.6141×10^{-9}	1.1640×10^{-7}	1.5053×10^{-10}	8.1921×10^{-8}
40	2.1100×10^{-12}	2.9068×10^{-8}	3.1103×10^{-13}	2.0470×10^{-8}

Table 6 Comparison of $||U||_\infty$ and $||U||_2$ norms with published results [25] for $\varepsilon = 0.005$, $\sigma = 100$ and $t = 0.001$

γ	Present method	[25]	Present method	[25]
	$\|\|U\|\|_\infty$	$\|\|U\|\|_\infty$	$\|\|U\|\|_2$	$\|\|U\|\|_2$
10	4.2175×10^{-8}	1.2150×10^{-7}	3.2446×10^{-8}	8.6310×10^{-8}
20	2.9029×10^{-10}	3.0620×10^{-8}	2.7071×10^{-11}	2.1530×10^{-8}
40	2.7000×10^{-13}	7.6440×10^{-9}	3.8863×10^{-14}	5.3780×10^{-9}

norms have been calculated for $\varepsilon = 0.005$, $\sigma = 100$ and $t = 0.001$. It has been distinguished from these tables that both Euclidean as well as supremum norms computed by QHCM are better than the norms estimated by modified cubic B-spline collocation method [25].

In Fig. 1 numerical solution is framed for different ε and at $t = 0.001$. The view of numerical solution has been demonstrated through surface plots given in Fig. 2. It can be easily seen from these graphs that numerical values are smooth which shows the efficiency and accuracy of QHCM.

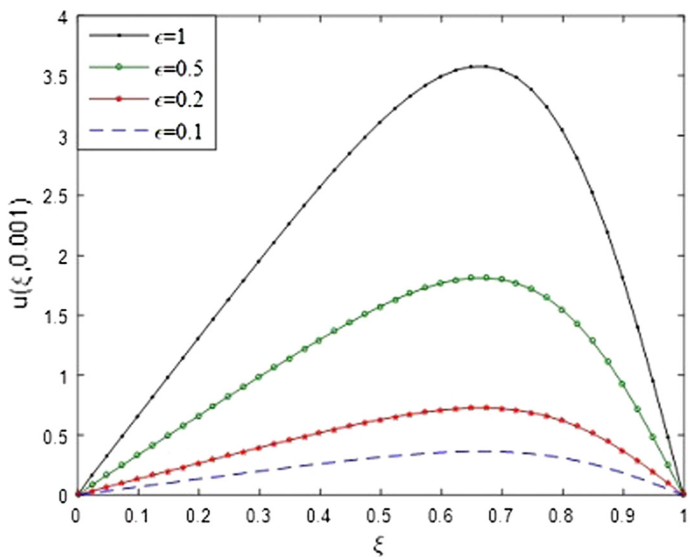

Fig. 1 Graphical view of the numerical solution for different ε, $\sigma = 2$ and $t = 0.001$ in the form of $2D$ plot

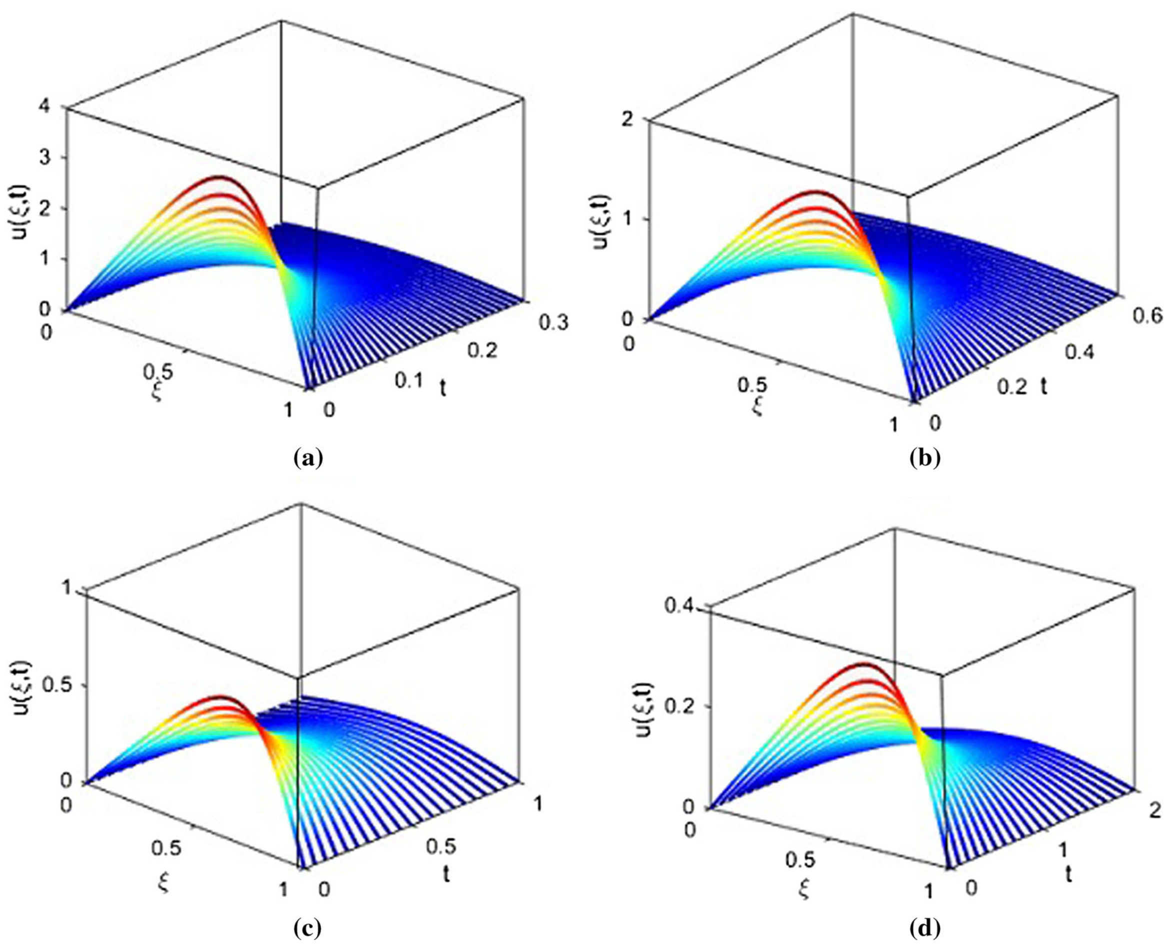

Fig. 2 Graphical view of the numerical solution for $\sigma = 2$ and **a** $\varepsilon = 1$ **b** $\varepsilon = 0.5$ **c** $\varepsilon = 0.2$ **d** $\varepsilon = 0.1$

Table 7 Comparison of numerical values with exact solution [25] at $t = 0.05$

ξ	$\varepsilon = 1 \times 10^{-5}$, $\vartheta_1 = 1 \times 10^{-5}$, $\vartheta_3 = 2$	Exact solution [25]	$\varepsilon = 1 \times 10^{-4}$, $\vartheta_1 = 1 \times 10^{-4}$, $\vartheta_3 = 2$	Exact solution [25]	$\varepsilon = 75 \times 10^{-5}$, $\vartheta_1 = 75 \times 10^{-5}$, $\vartheta_3 = 2$	Exact solution [25]
0.1	1.39376×10^{-5}	1.39376×10^{-5}	1.39377×10^{-4}	1.39377×10^{-4}	1.04537×10^{-3}	1.04534×10^{-3}
0.2	1.33510×10^{-5}	1.33510×10^{-5}	1.33511×10^{-4}	1.33510×10^{-4}	1.00137×10^{-3}	1.00134×10^{-3}
0.3	1.28340×10^{-5}	1.28340×10^{-5}	1.28340×10^{-4}	1.28340×10^{-4}	9.62582×10^{-4}	9.62561×10^{-4}
0.4	1.23777×10^{-5}	1.23777×10^{-5}	1.23778×10^{-4}	1.23778×10^{-4}	9.28360×10^{-4}	9.28343×10^{-4}
0.5	1.19747×10^{-5}	1.19747×10^{-5}	1.19748×10^{-4}	1.19747×10^{-4}	8.98130×10^{-4}	8.98115×10^{-4}
0.6	1.16183×10^{-5}	1.16183×10^{-5}	1.16183×10^{-4}	1.16183×10^{-4}	8.71391×10^{-4}	8.71378×10^{-4}
0.7	1.13026×10^{-5}	1.13026×10^{-5}	1.13026×10^{-4}	1.13026×10^{-4}	8.47712×10^{-4}	8.47701×10^{-4}
0.8	1.10226×10^{-5}	1.10226×10^{-5}	1.10227×10^{-4}	1.10226×10^{-4}	8.26714×10^{-4}	8.26704×10^{-4}
0.9	1.07741×10^{-5}	1.07741×10^{-5}	1.07741×10^{-4}	1.07741×10^{-4}	8.08070×10^{-4}	8.08062×10^{-4}

Table 8 Comparison of $\|U\|_\infty$ and $\|U\|_2$ norms with published results [25] at $t = 0.05$

ϑ_1	ε	ϑ_3	$\|U\|_\infty$		$\|U\|_2$	
			Present method	[25]	Present method	[25]
1×10^{-5}	1×10^{-5}	2	6.4620×10^{-12}	5.94×10^{-12}	5.6417×10^{-13}	3.29×10^{-12}
1×10^{-5}	1×10^{-5}	3	4.9180×10^{-12}	2.98×10^{-12}	4.2556×10^{-13}	1.70×10^{-12}
1×10^{-5}	1×10^{-5}	−2	8.9410×10^{-12}	1.12×10^{-11}	9.7343×10^{-13}	5.11×10^{-12}
1×10^{-5}	1×10^{-5}	−3	3.5640×10^{-12}	3.22×10^{-12}	3.1464×10^{-13}	1.33×10^{-12}
1×10^{-4}	1×10^{-4}	2	5.1246×10^{-10}	6.52×10^{-10}	6.2863×10^{-11}	3.24×10^{-10}
1×10^{-4}	1×10^{-4}	3	2.4044×10^{-10}	3.05×10^{-10}	3.0677×10^{-11}	1.58×10^{-10}
1×10^{-4}	1×10^{-4}	−2	8.3270×10^{-10}	1.11×10^{-9}	9.4430×10^{-11}	4.99×10^{-10}
1×10^{-4}	1×10^{-4}	−3	2.9141×10^{-10}	3.84×10^{-10}	2.8135×10^{-11}	1.54×10^{-10}
75×10^{-5}	75×10^{-5}	2	2.9265×10^{-8}	3.61×10^{-8}	3.5551×10^{-9}	1.82×10^{-8}
75×10^{-5}	75×10^{-5}	3	1.3909×10^{-8}	1.74×10^{-8}	1.7422×10^{-9}	8.94×10^{-9}
75×10^{-5}	75×10^{-5}	−2	4.6438×10^{-8}	6.23×10^{-8}	5.2934×10^{-9}	2.81×10^{-8}
75×10^{-5}	75×10^{-5}	−3	1.5968×10^{-8}	2.10×10^{-8}	1.5636×10^{-9}	8.50×10^{-9}

5.2 Problem

In this problem, the initial condition has been taken in terms of hyperbolic functions as given below:

$$u(x,0) = \vartheta_1 + \frac{\varepsilon\vartheta_2}{\cosh(x+\vartheta_3)} - \frac{\varepsilon \sinh(x)}{\cosh(x+\vartheta_3)}, \tag{22}$$

where ϑ_1, ϑ_2 and ϑ_3 are the parameters such that $\vartheta_2 = \sqrt{\vartheta_3^2 - 1}$. Boundary conditions have been taken to be Dirichlet's.

At jth collocation point and γth element, the initial and boundary conditions can be expressed as:

$$u(x_\gamma + \xi_j h_\gamma, 0) = \vartheta_1 + \frac{\varepsilon\vartheta_2}{\cosh(x_\gamma + \xi_j h_\gamma + \vartheta_3)} - \frac{\varepsilon \sinh(x_\gamma + \xi_j h_\gamma)}{\cosh(x_\gamma + \xi_j h_\gamma + \vartheta_3)}, \quad \forall \xi_j \in (0,1) \tag{23}$$

$$u(0,t) = 0 \quad \text{and} \quad u(1,t) = 0 \quad \forall\, t > 0. \tag{24}$$

The numerically obtained results have been juxtapositioned to the exact solution for distinct ranges of parameters. The comparison is shown in Table 7, from which it can be accomplished that numerical values agree well with the exact solution up to certain degree of accuracy. This fact authenticates the accuracy of QHCM.

The Euclidean as well as supremum norms have also been evaluated using Eqs. (16) and (17). Table 8 shows the comparison of these norms with published results of [25], for different ranges of parameters at $t = 0.05$. It has been analyzed that the norms figured by QHCM are better than [25]. In Fig. 3, numerical solution is organized for different values of parameters involved in the Burgers' equation and at $t = 0.05$. Figure 4 represents the view of numerical solution through surface plots. It can be perceived from these surface plots that numerical solution is smooth for all t and ξ and the values lie within the domain.

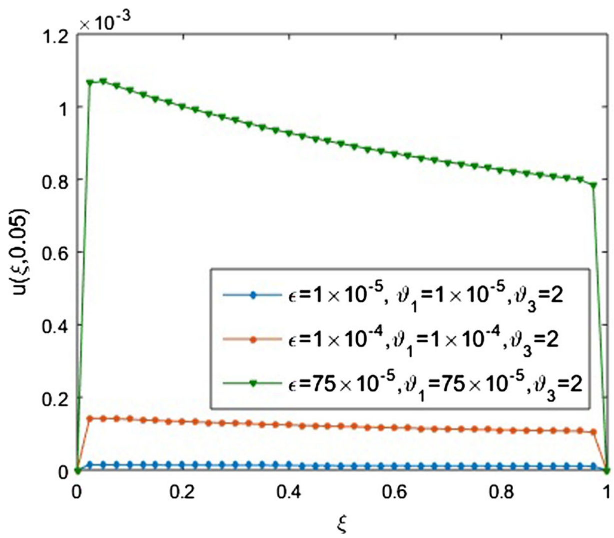

Fig. 3 Graphical view of solution for different ranges of parameters and $t = 0.05$

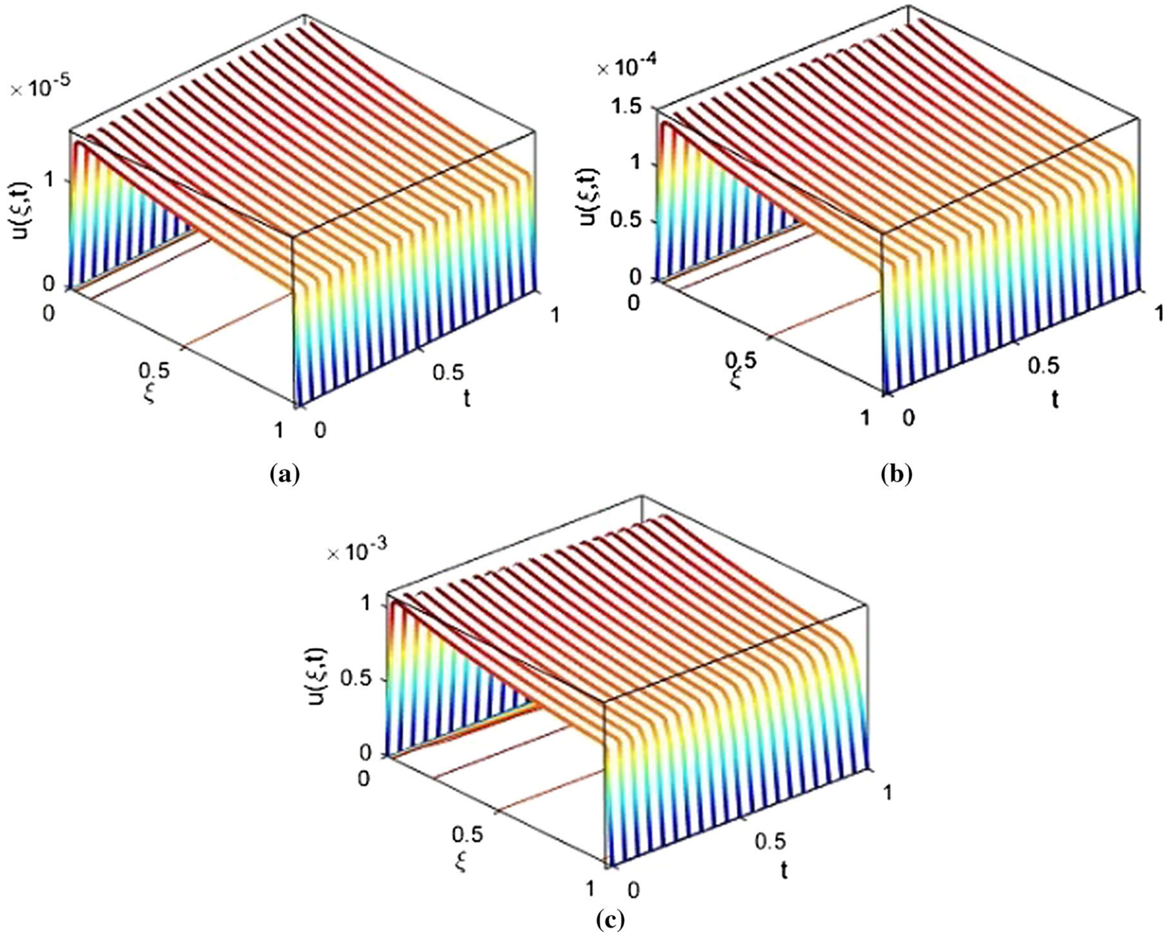

Fig. 4 Graphical view of the numerical solution for **a** $\varepsilon = 1 \times 10^{-5}$, $\vartheta_1 = 1 \times 10^{-5}$, **b** $\varepsilon = 1 \times 10^{-4}$, $\vartheta_1 = 1 \times 10^{-4}$, **c** $\varepsilon = 75 \times 10^{-5}$, $\vartheta_1 = 75 \times 10^{-5}$ and $\vartheta_3 = 2$

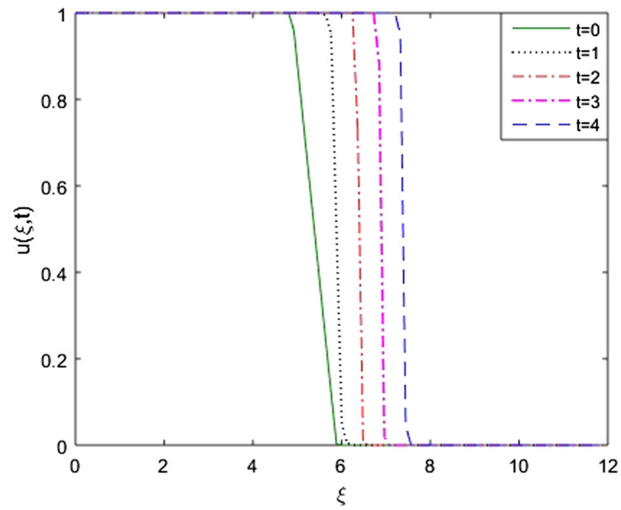

Fig. 5 Graphical view of solution for $\varepsilon = 0.01$ and t varies from 0 to 4

5.3 Problem

In this problem initial condition is defined as:

$$u(x,0) = \begin{cases} 1, & 0 \le x < 5 \\ 6 - x, & 5 \le x < 6 \\ 0, & 6 \le x < 12 \end{cases} \tag{25}$$

The boundary conditions are taken to be Dirichlet's.

At jth collocation point and γth element, the initial and boundary conditions can be expressed as:

$$u(x_\gamma + \xi_j h_\gamma) = \begin{cases} 1, & 0 \le \xi_j < 6 \\ 6 - (x_\gamma + \xi_j h_\gamma), & 5 \le \xi_j < 6 \\ 0, & 6 \le \xi_j < 12 \end{cases} \tag{26}$$

$$u(0,t) = 1 \quad \text{and} \quad u(12,t) = 0. \tag{27}$$

The results have been deliberated for varying values of ε. Numerically obtained results have been collated to the published results of [25] for $\varepsilon = 0.01$ and 0.1 in graphical form. Figure 5 shows the solution profiles for t varies from 0 to 4 and $\varepsilon = 0.01$. It can be noticed from this figure that the solution depicts same behavior as with the published result of [25] and are lying within the domain. Figure 6 shows the behavior of solution profiles for $\varepsilon = 0.1$. This figure is also compared to [25], and it is observed from this figure that the solution profiles show same configuration as in [25] and lie within domain. In Fig. 7, the solution profiles are manifested for t varies from 0 to 4 and $\varepsilon = 0.5$. The graphical view shows that the values lie within the domain. The numerical solution for varying ranges of ε has also been shown in terms of surface plots. The surface representation of these solution profiles is shown in Fig. 8.

5.4 Problem

Initial condition for this problem has been defined in terms of circular functions as:

$$u(x,0) = \begin{cases} \sin \pi x, & 0 \le x < 1 \\ -\frac{1}{2} \sin \pi x, & 1 \le x < 2 \\ 0, & 2 \le x < 5. \end{cases} \tag{28}$$

The boundary conditions are taken to be Dirichlet's.

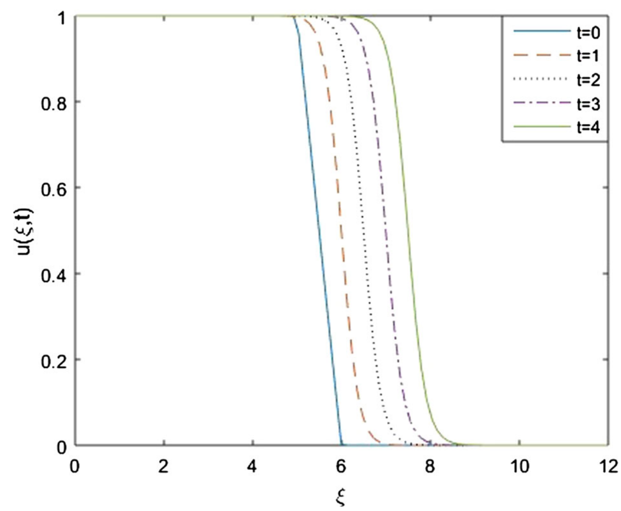

Fig. 6 Graphical view of solution for $\varepsilon = 0.1$ and t varies from 0 to 4

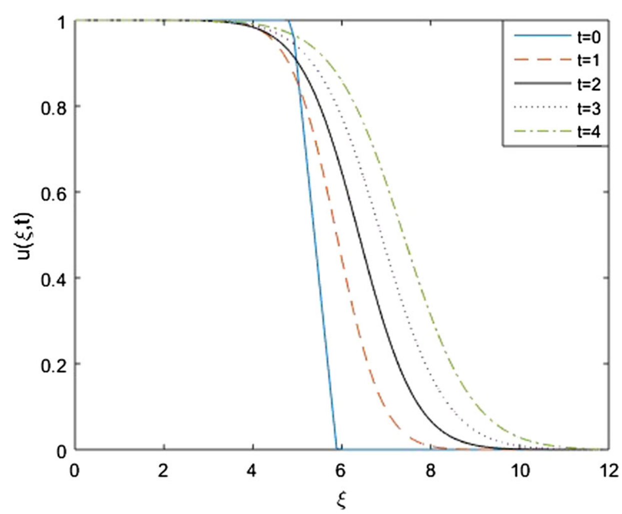

Fig. 7 Graphical view of solution for $\varepsilon = 0.5$ and t varies from 0 to 4

At jth collocation point and γth element, the initial and boundary conditions can be expressed as:

$$u(x_\gamma + \xi_j h_\gamma, 0) = \begin{cases} \sin \pi(x_\gamma + \xi_j h_\gamma), & 0 \le \xi_j < 1 \\ -\frac{1}{2} \sin \pi(x_\gamma + \xi_j h_\gamma), & 1 \le \xi_j < 2 \\ 0, & 2 \le \xi_j < 5 \end{cases} \tag{29}$$

$$u(0, t) = 0 \quad \text{and} \quad u(5, t) = 0. \tag{30}$$

The results have been reckoned for varying values of ε. Euclidean and supremum norms have been estimated using the formulas, $||U||_2 = \sqrt{\sum_{\gamma=1}^{ne} h_\gamma \sum_{i=1}^{6} w_i (u_i^\gamma)^2}$ and $||U||_\infty = max_{x_i} |u_i^\gamma|$, respectively $\forall\ i = 1, 2, \ldots, 6$ and $\gamma = 1, 2, \ldots, ne$, where u_i^γ represents the numerical solution obtained using quintic Hermite collocation method. These norms are presented in tabular form in Table 9. It can be seen from the table that both Euclidean and supremum norms lie within the domain.

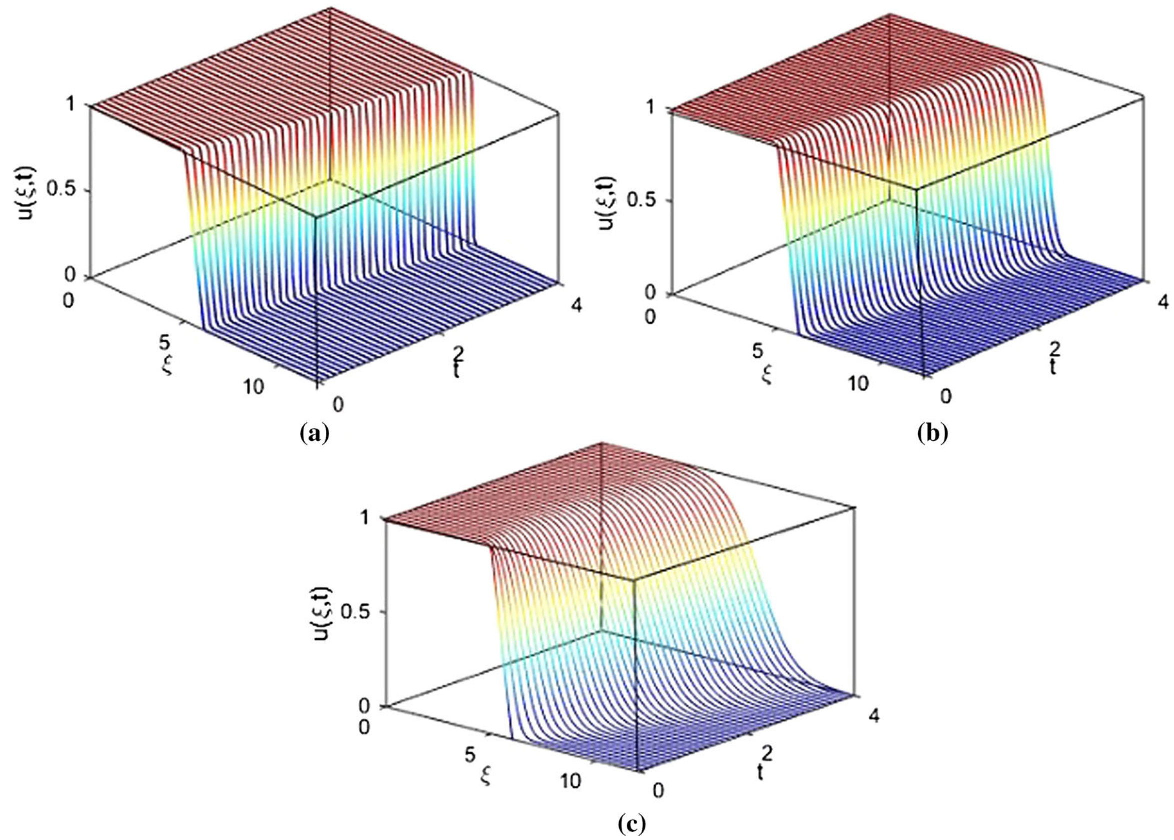

Fig. 8 Graphical view of solution for **a** $\varepsilon = 0.01$, **b** $\varepsilon = 0.1$, **c** $\varepsilon = 0.5$

Table 9 $||U||_\infty$ and $||U||_2$ norms for $\varepsilon = 0.01$ and 0.1

t	$\varepsilon = 0.01$		$\varepsilon = 0.1$	
	$\|\|U\|\|_\infty$	$\|\|U\|\|_2$	$\|\|U\|\|_\infty$	$\|\|U\|\|_2$
0	1.00000×10^{0}	7.37243×10^{-1}	1.00000×10^{0}	7.37243×10^{-1}
0.5	9.47863×10^{-1}	7.02060×10^{-1}	6.60785×10^{-1}	5.89624×10^{-1}
1.0	8.60633×10^{-1}	6.70406×10^{-1}	5.47454×10^{-1}	5.38305×10^{-1}
1.5	7.82716×10^{-1}	6.51156×10^{-1}	4.89309×10^{-1}	5.01773×10^{-1}
2.0	7.33314×10^{-1}	6.38737×10^{-1}	4.46073×10^{-1}	4.72214×10^{-1}
2.5	6.97992×10^{-1}	6.29428×10^{-1}	4.10694×10^{-1}	4.47586×10^{-1}
3.0	6.70299×10^{-1}	6.17321×10^{-1}	3.80972×10^{-1}	4.26714×10^{-1}
3.5	6.40990×10^{-1}	6.00419×10^{-1}	3.56068×10^{-1}	4.08767×10^{-1}
4.0	6.10163×10^{-1}	5.83079×10^{-1}	3.34664×10^{-1}	3.93139×10^{-1}
4.5	5.79422×10^{-1}	5.67320×10^{-1}	3.16124×10^{-1}	3.79375×10^{-1}
5.0	5.51924×10^{-1}	5.53283×10^{-1}	2.99897×10^{-1}	3.67132×10^{-1}

The numerical solution has also been computed for $\varepsilon = 0.01$ and 0.1. The results have been presented graphically in form of plane as well as surface plots. In Fig. 9 the behavior of solution profile is shown for $\varepsilon = 0.01$ and t varies form 0 to 10. Figure 10 represents the behavior of solution profiles for $\varepsilon = 0.1$. It can be observed from these figures that the solution profiles show the same configuration as in [25].

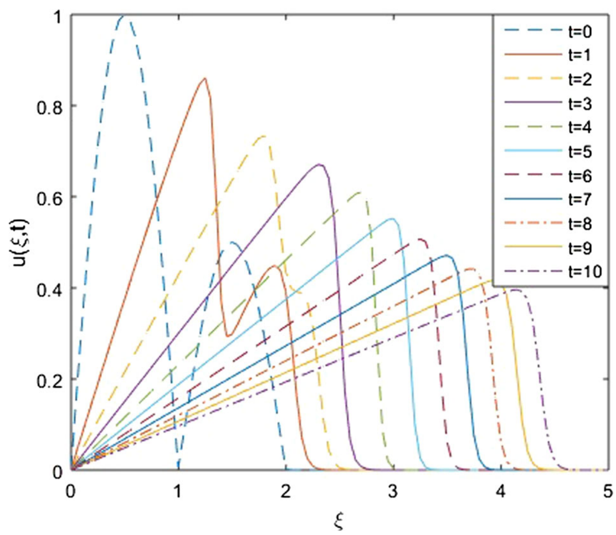

Fig. 9 Graphical view of solution for $\varepsilon = 0.01$ and t varies from 0 to 10

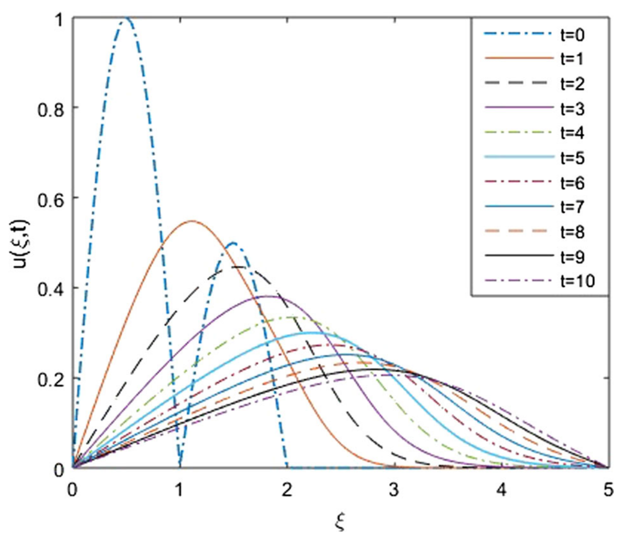

Fig. 10 Graphical view of solution for $\varepsilon = 0.1$ and t varies from 0 to 10

To view the solution in surface plots, the surface representation of the solution profiles is shown in Fig. 11. The surface view of the solution profiles shows the smoothness as well as the range of the solution profiles as the numerical solution lie within the domain.

5.5 Problem

In this problem, the initial condition has been defined in terms of exponential function as:

$$u(x, 1) = \frac{x}{1 + \exp\left[\frac{1}{4\varepsilon}\left(x^2 - \frac{1}{4}\right)\right]}. \tag{31}$$

The boundary conditions are taken to be Dirichlet's.

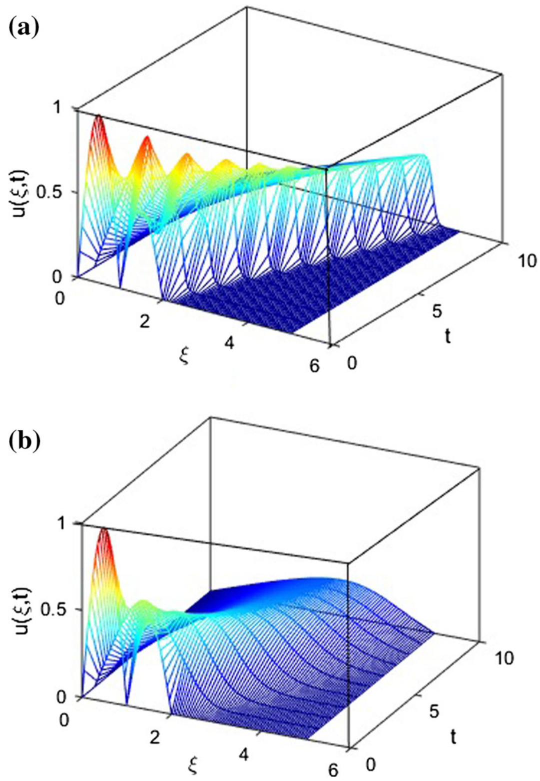

Fig. 11 Graphical view of solution for **a** $\varepsilon = 0.01$, **b** $\varepsilon = 0.1$

At jth collocation point and γth element, the initial and boundary conditions can be expressed as:

$$u(x_\gamma + \xi_j h_\gamma, 1) = \frac{x_\gamma + \xi_j h_\gamma}{1 + \exp\left[\frac{1}{4\varepsilon}\left((x_\gamma + \xi_j h_\gamma)^2 - \frac{1}{4}\right)\right]}, \quad \forall \xi_j \in (0, 1) \tag{32}$$

$$u(0, t) = 0 \quad \text{and} \quad u(1, t) = 0. \tag{33}$$

The proposed method has been followed to solve the Burgers' equation defined by Eq. (1). The results have been assessed for varying values of ε and presented in tabular and graphical form. The numerically obtained results with the proposed techniques have been compared to the exact solution and are presented in tabular form. Table 10 shows the comparison of exact solution to the numerical solution for $\varepsilon = 0.005$ and 0.01. From this table one can spot that numerical solution obtained from QHCM agrees well with the exact solution up to a certain degree of accuracy.

The Euclidean and supremum norms have been computed using the formulas given in Eqs. (16) and (17). These norms have been compared to the results of [25] and are presented in Table 11. It can be observed from this table that the norms are quite stable as compared to [25] up to certain a degree of accuracy. The numerically obtained results have been shown graphically through plane as well as surface plots. In Fig. 12, solution profiles are shown for $\varepsilon = 0.005$ at $t = 1$ to 4. Figure 13 represents the solution profiles for $\varepsilon = 0.01$ at $t = 1 - 4$. From these figures it is clear that the solution profiles lie within the domain. Figure 14 shows the solution profiles in surface representation.

6 Conclusions

The mechanism of quintic Hermite splines decodes the Burgers' equation directly without using Hopf–Cole transformation that converts it into linear form. The numerical solution of different problems with distinct initial conditions exhibits the accuracy of the QHCM. The numerically procured results have been collated to the exact solution and agrees well up to a certain degree of accuracy. A comparison has also been made with

Table 10 Comparison of exact and numerical values $\varepsilon = 0.005$ and 0.01

		$\varepsilon = 0.005$		$\varepsilon = 0.01$	
x	t	Exact	Present method	Exact	Present method
0.2	1.3	0.15384311	0.15384311	0.15311882	0.15311882
	1.7	0.11764521	0.11764521	0.11711621	0.11711618
	2.3	0.08695535	0.08695535	0.08656506	0.08656501
	2.7	0.07407312	0.07407312	0.07373533	0.07373529
	3.3	0.06060531	0.06060531	0.06031966	0.06031962
	3.7	0.05405339	0.05405339	0.05379232	0.05379229
0.4	1.3	0.30707837	0.30707695	0.29367117	0.29366962
	1.7	0.23516774	0.23516734	0.22922650	0.22922562
	2.3	0.17388120	0.17388110	0.17106221	0.17106181
	2.7	0.14813059	0.14813054	0.14610914	0.14610888
	3.3	0.12120285	0.12120283	0.11980026	0.11980009
	3.7	0.10810137	0.10810136	0.10693754	0.10693736
0.6	1.3	0.08576776	0.08576447	0.14266856	0.14266849
	1.7	0.29590968	0.29589363	0.23509176	0.23509084
	2.3	0.25722767	0.25722530	0.22752897	0.22752809
	2.7	0.22115808	0.22115723	0.20407618	0.20407531
	3.3	0.18153084	0.18153057	0.17256464	0.17256118
	3.7	0.16201159	0.16201144	0.15558382	0.15557318
0.8	1.3	0.00000295	0.00000295	0.00126027	0.00126027
	1.7	0.00064647	0.00064644	0.01480462	0.01480443
	2.3	0.04810368	0.04809479	0.08537726	0.08535181
	2.7	0.15935059	0.15933140	0.13539815	0.13523651
	3.3	0.21837411	0.21831121	0.16750249	0.16664677
	3.7	0.20772502	0.20771209	0.16886508	0.16888816

Table 11 Comparison of $||U||_\infty$ and $||U||_2$ with published results [25] for $\varepsilon = 0.005$ and $t = 3.6$

γ	Present method $\|\|U\|\|_\infty \times 10^3$	[25] $\|\|U\|\|_\infty \times 10^3$	Present method $\|\|U\|\|_2 \times 10^4$	[25] $\|\|U\|\|_2 \times 10^3$
20	1.17	2.56	1.09	1.02
30	1.17	1.56	0.89	0.53
40	1.17	1.00	0.77	0.31
60	1.18	0.47	0.64	0.15
80	1.19	0.27	0.56	0.08
100	1.18	0.17	0.49	0.06
120	1.18	0.12	0.42	0.04

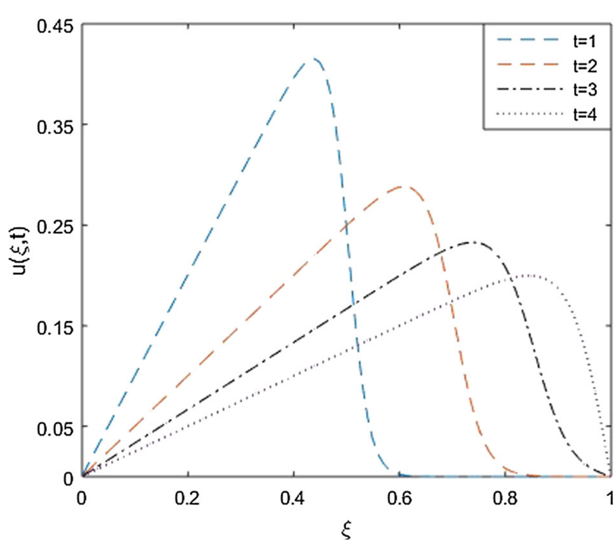

Fig. 12 Graphical view of solution for $\varepsilon = 0.005$ and t varies from 1 to 4

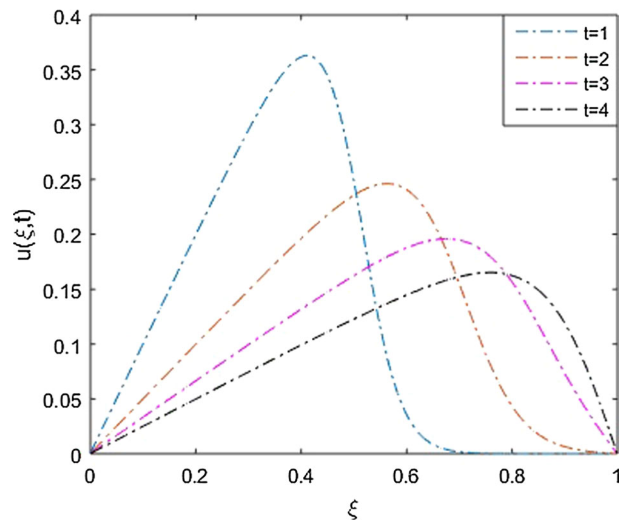

Fig. 13 Graphical view of solution for $\varepsilon = 0.01$ and t varies from 1 to 4

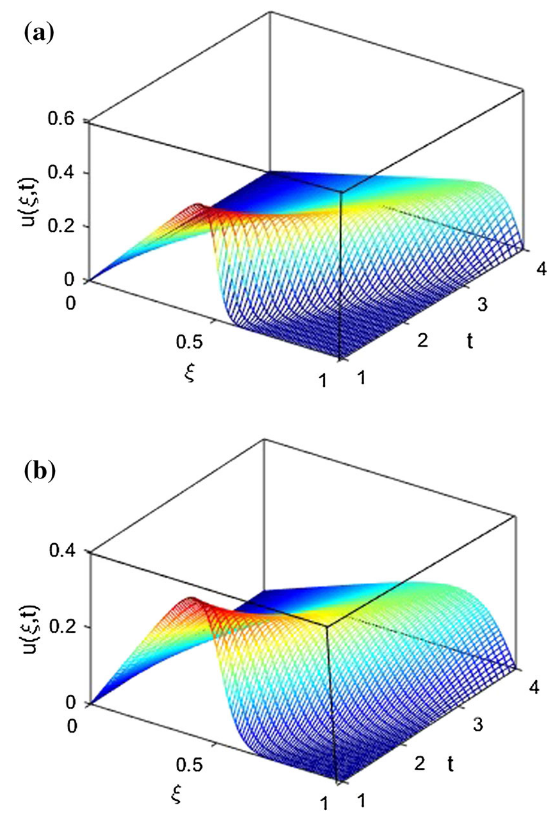

Fig. 14 Graphical view of solution for **a** $\varepsilon = 0.005$, **b** $\varepsilon = 0.01$

the published results. The enumeration and comparison of Euclidean and supremum norms show the efficiency as well as accuracy of the present procedure. It can be interpreted that the present technique is efficient up to a certain degree of accuracy as compared to modified cubic B-spline collocation method [25] and automatic differentiation method [7].

Acknowledgements Mrs. Inderpreet Kaur is thankful to DST for providing INSPIRE fellowship (IF140424).

References

1. Abbasbandy, S.; Darvishi, M.T.: A numerical solution of Burgers' equation by modified adomain method. Appl. Math. Comput. **163**, 1265–1272 (2005)
2. Aksan, E.N.: A numerical solution of Burgers' equation by finite element method constructed on the method of discretization in time. Appl. Math. Comput. **170**, 895–904 (2005)
3. Arora, S.; Kaur, I.: Applications of Quintic Hermite collocation with time discretization to singularly perturbed problems. Appl. Math. Comput. **316**, 409–421 (2018)
4. Arora, S.; Kaur, I.: An efficient scheme for numerical solution of Burgers' equation using quintic hermite interpolating polynomials. Arab. J. Math. **5**, 23–34 (2016)
5. Arora, S.; Kaur, I.; Potůček, F.: Modelling of Displacement washing of Pulp fibers using the Hermite collocation method. Br. J. Chem. Eng. **32**, 563–575 (2015)
6. Arora, G.; Singh, B.K.: Numerical solution of Burgers' equation with modified cubic B-spline differential quadrature method. Appl. Math. Comput. **224**, 166–177 (2013)
7. Asaithambi, A.: Numerical solution of the Burgers' equation by automatic differentiation. Appl. Math. Comput. **216**, 2700–2708 (2010)
8. Burger, J.M.: A mathematical model illustrating the theory of turbulence. Adv. Appl. Mech. **1**, 171–199 (1948)
9. Chen, F.; Wong, P.J.Y.: Error estimates for discrete spline interpolation: quintic and biquintic splines. J. Comput. Appl. Math. **236**, 3835–3854 (2012)
10. Cole, J.D.: On a quasi-linear parabolic equation occurring in aerodynamics. Q. Appl. Math. **9**, 225–236 (1951)
11. Dağ, İ.; Irk, D.; Saka, B.: A numerical solution of the Burgers' equation using cubic B-splines. Appl. Math. Comput. **163**, 199–211 (2005)
12. Dyksen, W.R.; Lynch, R.E.: A new decoupling technique for the Hermite cubic collocation equations arising from boundary value problems. Math. Comput. Simul. **54**, 359–372 (2000)
13. Finden, W.F.: Higher order approximations using interpolation applied to collocation solutions of two-point boundary value problems. J. Comput. Appl. Math. **206**, 99–115 (2007)
14. Gülsu, M.; Yalman, H.; Öztürk, Y.; Sezer, M.: A new Hermite collocation method for solving differential difference equations. Appl. Appl. Math. **6**, 1856–1869 (2011)
15. Hall, C.A.: On error bounds for spline interpolation. J. Approx. Theory **1**, 209–218 (1968)
16. Hopf, E.: The partial differential equation $u_t + uu_x = \nu u_{xx}$. Commun. Pure Appl. Math. **3**, 201–216 (1950)
17. Inc, M.: On numerical solution of Burgers' equation by homotopy analysis method. Phys. Lett. A **372**, 356–360 (2008)
18. Kadalbajoo, M.K.; Awasthi, A.: A numerical method based on Crank–Nicolson scheme for Burgers' equation. Appl. Math. Comput. **182**, 1430–1442 (2006)
19. Kutluay, S.; Esen, A.; Dag, I.: Numerical solutions of the Burgers' equation by the least-squares quadratic B-spline finite element method. J. Comput. Appl. Math. **167**, 21–33 (2004)
20. Kutluay, S.; Bahadir, A.R.; Özdeş, A.: Numerical Solution of one-dimensional Burgers equation: explicit and exact–explicit finite difference methods. J. Comput. Appl. Math. **103**, 251–261 (1999)
21. Lang, A.W.; Sloan, D.M.: Hermite collocation solution of near-singular problems using numerical coordinate transformations based on adaptivity. J. Comput. Appl. Math. **140**, 499–520 (2002)
22. Liao, W.: An implicit fourth-order compact finite difference scheme for one-dimensional Burgers' equation. Appl. Math. Comput. **206**, 755–764 (2008)
23. Liu, X.; Liu, G.R.; Tai, K.; Lam, K.Y.: Radial point interpolation collocation method (RPICM) for partial differential equations. Comput. Math. Appl. **50**, 1425–1442 (2005)
24. Ma, H.; Sun, W.; Tang, T.: Hermite spectral methods with a time-dependent scaling for parabolic equations in unbounded domains. SIAM J. Numer. Anal. **43**, 58–75 (2006)
25. Mittal, R.C.; Jain, R.K.: Numerical solutions of non-linear Burgers' equation with modified cubic B-splines collocation method. Appl. Math. Comput. **218**, 7839–7855 (2012)
26. Orsini, P.; Power, H.; Lees, M.: The Hermite radial basis function control volume method for multi-zones problems; A non-overlapping domain decomposition algorithm. Comput. Methods Appl. Mech. Eng. **200**, 477–493 (2011)
27. Özis, T.; Esen, A.; Kutluay, S.: Numerical solution of Burgers' equation by quadratic B-spline finite elements. Appl. Math. Comput. **165**, 237–249 (2005)
28. Pandey, K.; Verma, L.; Verma, A.K.: Du Fort-Frankel finite difference scheme for Burgers equation. Arab. J. Math. **2**, 91–101 (2013)
29. Ricciardi, K.L.; Brill, S.H.: Optimal Hermite collocation applied to a one-dimensional convection–diffusion equation using an adaptive hybrid optimization algorithm. Int. J. Numer. Methods Heat Fluid Flow **19**, 874–893 (2009)

30. Wood, W.L.: An exact solution for Burger' s equation. Commun. Numer. Methods Eng. **22**, 797–798 (2006)
31. Xu, M.; Wang, R.; Zhang, J.; Fang, Q.: A novel numerical scheme for solving Burgers' equation. Appl. Math. Comput. **217**, 4473–4482 (2011)
32. Yalçinbaş, S.; Aynigül, M.; Sezer, M.: A collocation method using Hermite polynomials for approximate solution of pantograph equations. J. Franklin Inst. **348**, 1128–1139 (2011)